Available online at www.sciencedirect.com
ScienceDirect
Journal of Controlled Release 119 (2007) 111 – 120
journal of controlled release
www.elsevier.com/locate/jconrel

A mechanistic model of controlled drug release from polymer millirods: Effects of excipients and complex binding

Fangjing Wang [a], Gerald M. Saidel [a,*], Jinming Gao [b]

[a] Department of Biomedical Engineering, Case Western Reserve University, Cleveland, OH 44106–7207, United States
[b] Simmons Comprehensive Cancer Center, University of Texas Southwestern Medical Center at Dallas, Dallas, TX 75390–8590, United States

Received 14 November 2006; accepted 29 January 2007
Available online 9 February 2007

Abstract

The incorporation of different cyclodextrin (CD) excipients such as HPβ–CD, β–CD, γ–CD or α–CD into polymer millirods for complexing β-lapachone (β-lap), a potent anti-cancer drug, significantly improved the drug release kinetics with various drug release patterns. However, such a complex system requires a mechanistically based model in order to provide a quantitative understanding of the many molecular events and processes that are essential for the rational development of millirod implants. This study focuses on mathematical modeling of drug release from PLGA cylindrical millirods. This millirod system incorporates multiple components: a PLGA matrix; excipient in free and complex forms; drug in free, bound, and crystalline forms. The model characterizes many dynamic transport and complexation processes that include radial diffusion, excipient complexation and crystalline drug dissolution. Optimal estimates of the model parameters were obtained by minimizing the difference between model simulation and experimentally measured drug release kinetics. The effects of different drug loadings on the drug release rate were simulated and compared with other data to validate this model. Whereas our model can simulate all the experimental data, the Higuchi model can simulate only some of them. Furthermore, our model incorporates mechanisms by which the processes underlying drug release from a polymer matrix can be quantitatively analyzed. These processes include drug entrapment/dissolution in the matrix, drug recrysallization, and supersaturation. This modeling study shows that complex binding capacity, which affects drug initial conditions, drug–polymer interactions, and bound drug behavior in aqueous solution, is crucial in controlling drug release kinetics.

Keywords: PLGA millirods; Mathematical model; Parameter estimation; Cyclodextrin inclusion complex; Excipients; Drug release

1. Introduction

Site-specific, controlled release of cytotoxic agents from biodegradable polymer drug delivery systems implanted in solid tumors has advantages over systemic drug therapy. Tumors can be directly exposed to therapeutic levels of the drug for a sustained period with reduced systemic toxicity [1]. Drug inclusion in a polymer depot allows for tailoring of release kinetics to achieve the most efficacious delivery regimen. As described previously, a polymeric drug device has been developed in the form of a cylindrical millirod composed of poly(D,L-lactide-*co*-glycolide) (PLGA) that can be implanted within a solid tumor for delivery of anticancer agents [2]. Studies with these devices have examined the control of drug release [3,4] and drug transport in tissues [3,5,6]. Implantation of millirods in rabbit VX-2 liver tumors with doxorubicin has shown efficacious anti-tumor response [7]. Local delivery of dexamethasone through millirod implants effectively decreased fibrous capsule formation in ablated liver tissues compared with systemic (i.p. injection) administration [8].

A naturally occurring 1,2-naphthoquinone, β-lapachone (β-lap) [9], has demonstrated specific anti-cancer activity against a wide variety of tumors [10]. The unique mechanism of β-lap action derives from the expression of the cytosolic enzyme, NAD(P)H:quinone oxidoreductase-1 (NQO1) [11]. This enzyme is endogenously elevated in tumor cells (up to 20-fold) compared to adjacent normal cells [12]. Furthermore, β-lap has distinct advantages over other chemotherapeutic

* Corresponding author. Tel.: +1 216 368 4066; fax: +1 216 368 4969.
E-mail address: gerald.saidel@case.edu (G.M. Saidel).

0168-3659/$ - see front matter © 2007 Elsevier B.V. All rights reserved.
doi:10.1016/j.jconrel.2007.01.019

agents in that it kills tumors independent of p53 status, cell cycle state, caspases, while inducing a novel μ-calpain-mediated apoptotic response [11,13,14]. In particular, this drug shows superiority in treating slowly dividing cancer cells in breast, lung or prostate tissue, whereas most current drugs are more effective in killing fast growing tumors. Synergistic action of β-lap with taxol, DNA damaging agents and ionization radiation has been effective against tumors [15,16]. Since β-lap is hydrophobic, inclusion complexes have been made for effective administration [17]. Further development of a controlled delivery system is needed for this anti-cancer agent to have significant therapeutic value.

Recently, PLGA millirods have been developed for the local delivery of β-lap [18]. Due to the low aqueous solubility (0.04 mg/mL) of β-lap [17], its release rate from PLGA millirods was not sufficient. The use of inert excipients such as glucose into the millirods improved the drug release rate to a limited extent. A significant improvement in the drug release rate was obtained by incorporating hydrophilic cyclodextrins (CD) into the PLGA matrix (i.e., β-lap/CD inclusion complexes). The cyclic oligosaccharide CDs consist of a hydrophobic core and a hydrophilic outer surface [19,20], and can form inclusion complexes with β-lap, which subsequently increases the apparent water solubility of the drug [17]. These CDs differ in the number of glucopyranose units (6, 7, 8 for α–, β–, γ–CDs), complexing capability and water solubility [17]. In particular, hydroxypropyl-β–cyclodextrin (HPβ–CD) is obtained by treating a base-solubilized solution of β–CD with propylene oxide, resulting in a CD with greater solubility (~500 vs. 18.5 mg/ml at 25 °C). With respect to the varied drug release patterns achieved by these CDs, many factors may be involved: water permeation rates inside the polymer; pore formation; distribution of drug among different states (e.g., dissolved within PLGA matrix, complexed with CDs, or crystalline); drug binding capacities with different CDs; solubility and diffusivity of drug or drug–CD complexes; and dissolution kinetics of drug and drug–CD complexes.

For this complex system, a quantitative analysis of the different kinetic processes during drug release is necessary to rationally design optimal millirod formulations with controllable release kinetics. In this study, a mechanistic mathematical model was developed to predict the drug release behavior from an implanted polymer millirod with various drug/excipient combinations. This model incorporates the essential transport and kinetic processes underlying the drug release from the polymeric millirods. This quantitative approach provides a firm basis for the design of new polymeric drug-delivery systems by simulating the effects of the composition and geometry on drug release kinetics.

2. Experimental studies

Most of the experimental data in this study are available from a previous study that provides the detailed description of the materials and experimental procedures [18]. Therefore, only a brief summary is given here. Cylindrical polymer millirods (1.6 mm in diameter, 10 mm long) composed of PLGA matrix, β-lap, and an excipient were prepared by a compression–heat molding method at 90 °C for 2 h. β-Lap release experiments were performed in a well-mixed solution of 10 ml PBS at 37 °C, and drug concentration was measured via UV–Vis at its maximum adsorption wavelength (λ_{max} = 258 nm). Differential scanning calorimetry (Perkin Elmer DSC-7, Boston, USA) was used to measure the free β-lap content in the millirod CD/β-lap complex or physical mixture.

3. Model development and simulation methods

3.1. Transport and release mechanisms

After a millirod is placed into PBS solution, water permeates into it and dissolves CD, CD/β-lap complex and the crystalline drug. This produces pores that become immediately occupied by water, which allows diffusion of the dissolved drug and excipient from the millirod into the PBS (Fig. 1). Fig. 2 shows a system diagram for the drug release from the millirods with CD. No drug binding occurs when glucose is the excipient, which simplifies the system. Drug, excipient, and their complex are assumed to be uniformly distributed in the millirod. The crystalline free β-lap dissolves in water at a slower rate than CD/β-lap complex. If the local concentration of free β-lap in water becomes sufficiently large, then it can form a solid crystal. In the liquid phase, the binding interaction of CD and β-lap forms a 1:1 inclusion complex [17], which is reversible:

$$\text{Free drug(dissolved in water)} + \text{CD} \underset{k_2}{\overset{k_1}{\rightleftharpoons}} \text{Complex(bound drug)}$$

In the millirod, a fraction of drug can be entrapped or dissolved in the PLGA matrix as shown by DSC [18]. Drug release from this fraction will be slower than drug release through the pores and channels.

During the experimental period, PLGA polymer degradation process is negligible and the millirod remains intact. For a large ratio of length to radius (L/R = 12.5 > 10), the end effects are expected to be negligible, the dominant rate processes take place in the radial direction. In the solid phase of the millirod, the free drug, the bound excipient/drug complex, and the free excipient occupy volume fractions F_β, $F_{\beta e}$, F_e, respectively. Within the millirod, the water concentration $C_w(r,t)$ at any radial position and time reflects the local porosity. Given the water concentration in solution surrounding the millirod, the maximum water concentration within the millirod is $(F_\beta+F_{\beta e}+F_e)C_w^+$. Subsequently, the maximum pore density in the millirod can be

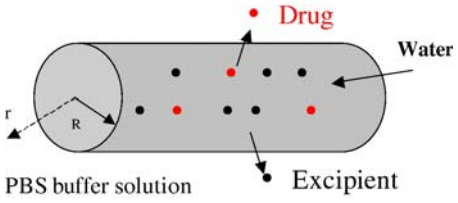

Fig. 1. Diagram of the millirods.

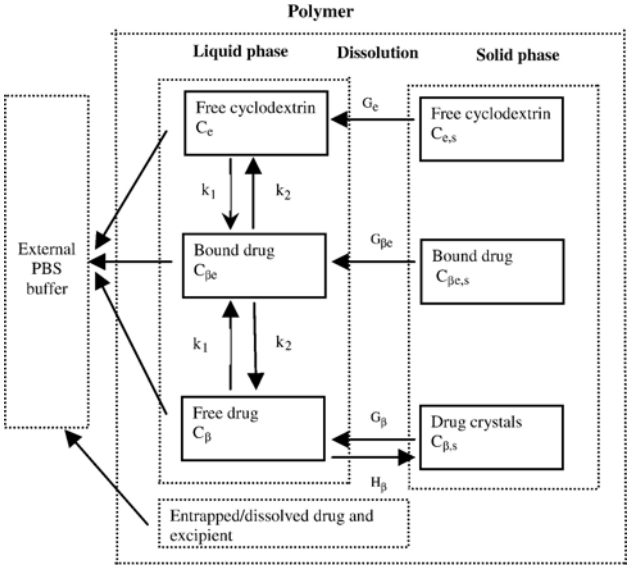

Fig. 2. System diagram for the drug release from the millirods. In the diagram, C_e, C_β, $C_{\beta e}$ are the concentrations of the free excipient, free drug, and bound drug in the solution, respectively. $C_{e,s}$, $C_{\beta,s}$, $C_{\beta e,s}$ are the solid concentrations of the excipient, crystalline drug, and bound excipient in the millirod, respectively. G_e, G_β, $G_{\beta e}$ are the dissolution rate of the free excipient, crystalline drug, and bound drug in the solution, respectively. H_β is the drug recrystallization rate. $C_e^{\max}$, $C_\beta^{\max}$, $C_{\beta e}^{\max}$ are the maximum concentration of the free excipient, free drug, and bound drug in the solution, respectively. $\gamma_{e,s}$, $\gamma_{\beta,s}$, $\gamma_{\beta e,s}$ are the dissolution rate constant of the free excipient, free drug, and bound drug, respectively. k_1 is the complex formation rate, and k_2 is the complex dissociation rate. C_i^* is the concentration of the entrapped drug or excipient or bound drug, $i = \beta, \beta e, e$.

evaluated as: $(F_\beta+F_{\beta e}+F_e)C_w^+ \cong F_\beta+F_{\beta e}+F_e$ for $C_w^+ \approx 1$ g/ml. (when glucose is the excipient, $F_{\beta e} = 0$).

3.2. Mass transport dynamics

3.2.1. Water transport and pore formation

From a phenomenological perspective, we can consider the water concentration within the millirod, which can represent pore density, to diffuse radially according to

$$\frac{\partial C_w}{\partial t} = \frac{1}{r}\left[\frac{\partial}{\partial r}\left(rD_w\frac{\partial C_w}{\partial r}\right)\right], \quad 0 \le r < R$$

We assume that the water (or pore) diffusion coefficient is proportional to the pore density: $D_w = \alpha C_w$. When water concentration is zero, the diffusion coefficient would vanish. When no excipient is used, porosity does not change so that D_w is assumed to be constant. Greater porosity provides more surface area for dissolution and a higher effective diffusion coefficient. At the surface of the millirod, where the dissolution is expected to reach the maximum extent, the boundary condition is

$$r = R: \; C_w = \left(F_\beta + F_{\beta e} + F_e\right)C_w^+ (0 < t)$$

At the center of the millirod, symmetry prevails:

$$r = 0: \; \partial C_w/\partial r = 0 \quad (0 < t)$$

Initially, there is no water in the millirod:

$$t = 0: C_w = 0 \quad (0 \le r < R)$$

3.2.2. Concentration distribution dynamics within millirods

In the millirod liquid phase, processes of most free drug, complex, and free excipient $i \in (\beta, \beta e, e)$ include diffusion through pores, dissolution from the solid-phase G_i, crystallization from solution H_i, and chemical reaction of the complex ϕ_i (M/h):

$$\frac{\partial C_i}{\partial t} = \frac{1}{r}\left[\frac{\partial}{\partial r}\left(rD_i\frac{\partial C_i}{\partial r}\right)\right] + G_i - H_i + \phi_i \mathrm{MW}_i, \quad 0 \le r < R$$

where the diffusion coefficient is proportional to the pore density (or water concentration) $D_i = \beta_i C_w$ and $D_e \approx D_{\beta e}$. MW_i denotes the molecular weight of component i. When no excipient is used, porosity does not change so that D_i is assumed to be constant. The crystallization occurs only for free drug, i.e., $H_i = 0$ for $i \in (e, \beta e)$. The net reaction rate for each component is

$$\phi_\beta = -k_1 C_\beta C_e / \left(\mathrm{MW}_\beta \mathrm{MW}_e\right) + k_2 C_{\beta e}/\mathrm{MW}_{\beta e} = \phi_e = -\phi_{\beta e}$$

The solution surrounding the millirod has a relatively large and well-mixed volume so the concentrations of all the dissolved species at the outer surface are negligible:

$$r = R: \quad C_i = 0$$

By symmetry at the center of the millirod,

$$r = 0: \quad \partial C_i/\partial r = 0 \quad (0 < t)$$

Initially within the millirod, there is no solution or dissolved species:

$$t = 0: \quad C_i = 0 \quad (0 \le r < R)$$

(when glucose is the excipient, $\phi_i = 0$ i $\in (\beta, e)$.)

3.2.3. Concentration distribution dynamics of entrapped/dissolved components

In this case, the three components $i \in (e, \beta e, \beta)$ are assumed to diffuse in the millirod with a small diffusion coefficient D_i^* independent of porosity changes:

$$\frac{\partial C_i^*}{\partial t} = \frac{1}{r}\left[\frac{\partial}{\partial r}\left(\frac{rD_i^*\partial C_i^*}{\partial r}\right)\right], \quad 0 \le r < R$$

It is assumed that the trapped or dissolved components will eventually disappear into solution surrounding the millirod:

$$r = R: \; C_i^* = 0$$

By symmetry at the center of the millirod,

$$r = 0: \partial C_i^*/\partial r = 0$$

Initially, we assume that a small fraction F_i^* of the concentration of each component is entrapped:

$$t = 0: \quad C_i^* = F_i^* C_{i,s}^0$$

(when glucose is the excipient, $i \in (\beta, e)$).

3.2.4. Interphase processes

Within the millirod solid phase, the initial concentrations of drug, excipient, and complex are specified:

$$t = 0: \quad C_{i,s} = C_{i,s}^0 \quad i \in (e, \beta e, \beta)$$

(when glucose is the excipient, $i \in (\beta, e)$).

At any later time, the concentration $C_{i,s}(r,t)$ $i \in (e, \beta e)$ of free or bound excipient at any position in the solid phase is lost by dissolution at rate $G_i(r,t)$

$$\frac{\partial C_{i,s}}{\partial t} = -G_i = -\gamma_{i,s}\left[C_i^{\max} - C_i\right] C_w C_{i,s} \quad \text{for} \quad C_i^{\max} > C_i$$

The rate of dissolution depends on the solubility or the maximum concentration in solution $C_i^{\max}$, the surface area between the solid excipient and water phases as indicated by the pore density C_w, and the solid-phase concentration $C_{i,s}$. The dissolution rate is zero when water concentration (or pore density) vanishes, the solution is saturated, or all local free or bound excipient has been lost from the solid phase.

Table 1
Parameters with known values

Model symbols	Parameters	Value	Remarks
α($cm^5 h^{-1} mg^{-1}$)	Coefficient for water penetration	5.0×10^{-6}	All excipients
$C_{\beta e}^{\max} = C_e^{\max}$ (mg/ml)	Excipient solubility	710 [a]	HPβ–CD
		30.6 [b]	β–CD
		406 [b] (200 [c] for complex)	γ–CD
		220 [b]	α–CD
		910 [d]	Glucose
$C_\beta^{\max}$(mg/ml)	Drug solubility	0.04	β-lap
C_β^{thresh} (mg/ml)	Threshold for recrystallization	0.11	For all CDs
$F_\beta + F_{\beta e} + F_e$	Porosity occupied by excipients and drug	0.45	Estimated from the water uptake data
F_i^*	Fraction of drug entrapped/dissolved	0.3	All excipients
k_1($M^{-1} h^{-1}$)	Forward complexation rate	2×10^3	All CDs
L(cm)	Millirod length	1.0	
MW (Da)	Molecular weight	1400	HPβ–CD
		1135	β–CD
		1297	γ–CD
		972	α–CD
		242	β-lap
R(cm)	Millirod radius	0.08	
$\gamma_{\beta e,s} = \gamma_{e,s}$ ($ml^2 mg^{-2} h^{-1}$)	Coefficient for excipient dissolution [e]	2.5×10^{-5}	HPβ–CD
		5.6×10^{-4}	β–CD
		4.2×10^{-5}	γ–CD
		7.7×10^{-5}	α–CD
		1.9×10^{-5}	Glucose
$\gamma_{\beta,s}$ ($ml^2 mg^{-2} h^{-1}$)	Coefficient for drug dissolution	1.2×10^{-2}	Estimated from lab experiments
γ_β(h^{-1})	Coefficient for drug recrystallization	2.0×10^3	All excipients

[a] Obtained from literature [22].
[b] Estimated based on literature [23].
[c] γ–CD/β-lap complex has decreased solubility at higher γ–CD concentration [17].
[d] Solubility at 25 °C.
[e] Estimate based on literature [21].

Table 2
Parameters from optimal estimation by model fitting to the experimental data

Model symbols	Parameters	Value	Remarks
D_i^*($cm^2 h^{-1}$)	Diffusion coefficient for drug entrapped/dissolved	$(2.6 \pm 0.4) \times 10^{-6}$	HPβ–CD, β–CD, γ–CD complex
		$(4.5 \pm 7.8) \times 10^{-7}$	HPβ–CD/drug mixture, glucose, α–CD
k_2 (h^{-1})	Backward complexation rate	2.5±0.01	HPβ–CD
		2.5±0.01	β–CD
		40.0±0.01	γ–CD
		133.3±0.02	α–CD
β_β ($cm^5 h^{-1} mg^{-1}$)	Coefficient for drug diffusion	$(7.5 \pm 1.7) \times 10^{-7}$	CD formulations
		$(5.8 \pm 1.1) \times 10^{-8}$	Glucose
D_β ($cm^2 h^{-1}$)	Drug diffusion coefficient	$(8.4 \pm 0.6) \times 10^{-7}$	No excipient
$\beta_{\beta e} = \beta_{\beta e}$ ($cm^5 h^{-1} mg^{-1}$)	Coefficient for excipient diffusion process	$(4.9 \pm 0.2) \times 10^{-7}$	HPβ–CD
		$(2.5 \pm .08) \times 10^{-7}$	β–CD
		$(1.5 \pm 1.2) \times 10^{-7}$	γ–CD
		$(2.8 \pm 0.4) \times 10^{-7}$	α–CD

In contrast, the free drug concentration $C_{\beta,s}(r,t)$ in the solid phase of the millirod can be lost by dissolution at rate $G_\beta(r,t)$ and gained by crystallization at rate $H_\beta(r,t)$:

$$\frac{\partial C_{\beta,s}}{\partial t} = H_\beta - G_\beta$$

The free drug re-crystallizes above a threshold:

$$H_\beta = \gamma_\beta\left[C_\beta - C_\beta^{\text{thresh}}\right] \quad \text{for} \quad C_\beta > C_\beta^{\text{thresh}}$$

When its concentration is below the threshold, it dissolves similarly to the excipient:

$$G_\beta = \gamma_{\beta,s}\left[C_\beta^{\text{thresh}} - C_\beta\right] C_w C_{\beta,s} \quad \text{for} \quad C_\beta^{\text{thresh}} > C_\beta$$

3.2.5. Model outputs for comparison with data

The cumulative drug released (represented by equivalent free drug amount) in the time interval (0, t) is the difference in the total amount of drug loaded initially $M_{\beta,\beta e}^0$ (equivalent total amount of free drug) and that remaining in the millirod:

$$M_{\beta,\beta e}(t) = M_{\beta,\beta e}^0 - 2\pi L \int_0^R r\Big[C_\beta + C_{\beta,s} + C_\beta^* + \frac{\text{MW}_\beta}{\text{MW}_{\beta e}}\left(C_{\beta e} + C_{\beta e,s} + C_{\beta e}^*\right)\Big] dr$$

The cumulative mass loss of drug and excipient by the millirod in the time interval (0,t) is:

$$M_{\beta,\beta e,e}(t) = M_{\beta,\beta e,e}^0 - 2\pi L \sum_i \int_0^R r\left[C_i + C_{i,s} + C_i^*\right] dr, \; i \in (\beta, \beta e, e)$$

Table 3
Millirod formulations and initial conditions (total content of drug/excipient, and PLGA are kept at 40% and 60%, respectively in all cases)

Experiments	Drug loading (%)	Free drug $C_{\beta,s}(0)$ (mg/ml)	Bound drug $C_{\beta e,s}(0)$ (mg/ml)	Excipient $C_{e,s}(0)$ (mg/ml)	Remarks
No excipient	1.2	11.9	0.0	0.0	
Glucose	1.2	11.9	0.0	386.1	Interaction with PLGA or drug neglected
HPβ–CD mixture	1.2	11.9	0.0	386.1	No bound drug formation
HPβ–CD complex	1.2	0.0	81.0	317.0	From DSC results
HPβ–CD complex	1.8	0.0	121.5	276.5	From DSC results
β–CD complex	1.8	0.0	101.9	296.2	From DSC results
γ–CD complex	1.8	0.0	113.9	284.1	From DSC results
α–CD complex	1.8	8.9	44.8	344.4	Calculated from DSC results
HPβ–CD complex	3.0	0.0	202.6	195.5	From DSC results
HPβ–CD complex	6.0	32.3	186.2	179.5	Calculated from DSC results
HPβ–CD complex	10.0	75.3	164.2	158.6	Calculated from DSC results

3.3. Model simulation and parameter estimation

The nonlinear system of differential equations was solved numerically using the "pdepe" in MATLAB. Some parameters of this system were evaluated from previous experimental studies (Table 1) [21–23], whereas other parameters in Table 1 such as F_i^*, α, k_1, γ_β, C_β^{thresh} were set based on simulations of our experimental data, and assumed to have the same values in all experiments. As a preliminary step in estimating the unknown parameters in Table 2, simulations were performed to investigate the effects of different parameters and determine a reasonable range of values for each parameter. With these ranges as constraints, optimal estimates of the parameters were obtained to provide the best least-squares fit of the model output to the experimental data using "lsqcurvefit" in MATLAB. The standard deviations and correlation coefficients of the parameter values were calculated via Jacobian values from "lsqcurvefit". Since millirods of HPβ–CD complex (1.2% and 1.8% drug loading) and HPβ–CD mixture only differ in their initial conditions (Table 3), data from these experiments were first used to evaluate parameter values for k_2, β_β, β_e (= $\beta_{\beta e}$) and D_i^*. The estimated values of some parameters (viz., β_β and D_i^*) obtained from HPβ–CD data would be expected to be close to the optimal parameter estimates from other similar data, and were used as common parameter values in the estimation of parameters in other formulations.

4. Results

4.1. Optimal estimation of model parameters

The data sets used to validate the model deal with the effects on β-lap release studies from the millirods of different formulations [18]. Optimal estimates of the parameters (Table 2) were obtained that allow the model to closely simulate these data (Figs. 3, 4). In addition, the standard deviations of the estimated parameters were relatively small (Table 2). The data shown in Fig. 3 come from experiments with either HPβ–CD/β-lap complex, HPβ–CD/β-lap mixture, or glucose, or without excipient. These dynamic responses show that drug release rate was slowest when no excipient was incorporated into the millirod. Incorporation of glucose into

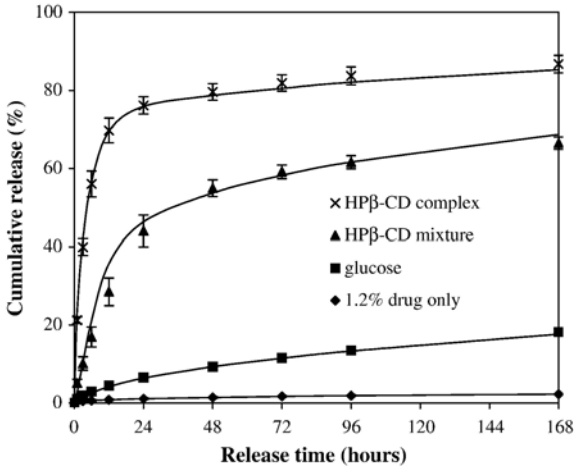

Fig. 3. β-Lap release profiles from millirods incorporated with HPβ–CD complex, HPβ–CD mixture, glucose, and no excipient, respectively ($n = 3$). The cumulative drug release refers to total β-lap including the free and bound forms. For simplicity, the total is represented by the equivalent amount of free drug. The drug loading used was 1.2%. The complex or excipient weight ratio with respect to PLGA was 40:60. The symbols represent the experimental data with standard deviations, and the lines represent model simulations with optimal parameter estimates.

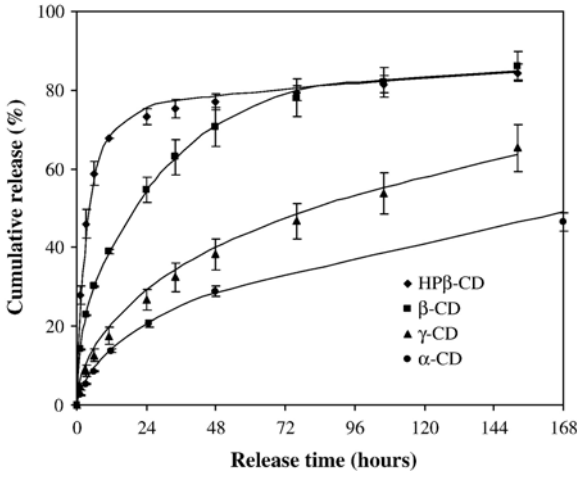

Fig. 4. β-Lap release from millirods incorporated with different cyclodextrins ($n = 3$). The cumulative drug release refers to total β-lap including the free and bound forms. For simplicity, the total is represented by the equivalent amount of free drug. The complex weight ratio with respect to PLGA was kept at 40:60. Drug loading used was 1.8%. The symbols represent the experimental data with standard deviations, and the lines represent the model simulations with optimal parameter estimates.

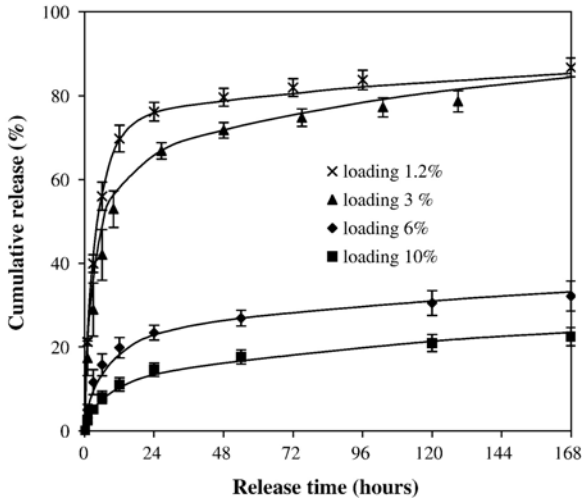

Fig. 5. β-Lap release profiles from millirods incorporated with HPβ–CD complex with varied drug/CD ratios (n = 3). The cumulative drug release refers to total β-lap including the free and bound forms. For simplicity, the total is represented by the equivalent amount of free drug. The complex/PLGA ratio was kept at 40:60. The symbols represent the experimental data with standard deviations, and the lines represent the model simulations with optimal parameter estimates.

millirods led to a significantly improved drug release rate, but the total amount of drug release may not be sufficient for therapeutic use. The fastest release rate was obtained with the HPβ–CD complex in the millirods.

Furthermore, the model could simulate the effect of different CD complexes incorporated into the millirods (Fig. 4). These

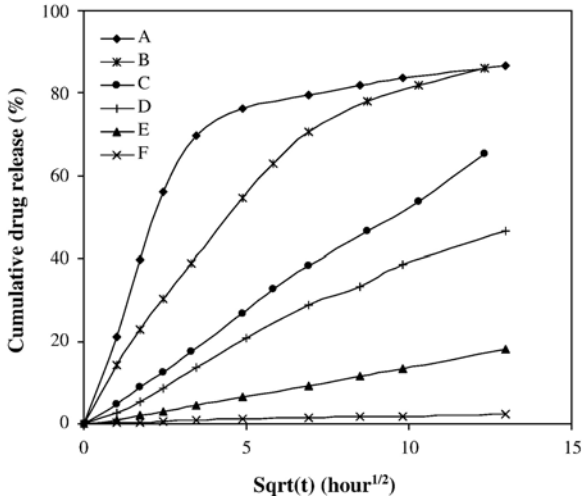

Fig. 6. A comparison with the conventional Higuchi model by re-plotting the cumulative drug release rate versus the square root of the time (hours). The cumulative drug release refers to total β-lap including the free and bound forms. For simplicity, the total is represented by the equivalent amount of free drug. The millirods were incorporated with: A) HPβ–CD complex, 1.2% drug loading B) β–CD complex, 1.8% drug loading C) γ–CD complex, 1.8% drug loading D) α–CD complex, 1.8% drug loading E) glucose, 1.2% drug loading F) no excipient, 1.2% drug loading, respectively. Similar β-lap release patterns with two distinct phases from millirods incorporated with HPβ–CD mixture (1.2% drug loading), as well as with HPβ–CD complex with varied drug loadings (3%, 6% and 10%) were obtained (data not shown).

have varied binding affinities and release kinetics. DSC showed that the solid inclusion complex incorporated into these millirods containing HPβ–CD, β–CD and γ–CD was fully amorphous, whereas ~50% β-lap was still in crystalline form in the α–CD solid inclusion complex (Table 3). The drug release rate followed in the order: HPβ-CD > β–CD > γ–CD > α–CD.

4.2. Predicting effects of drug loadings

To verify whether the mechanistic mathematic model developed in this study can be used for prediction analyses, the release rates of different drug/cyclodextrin ratios of the

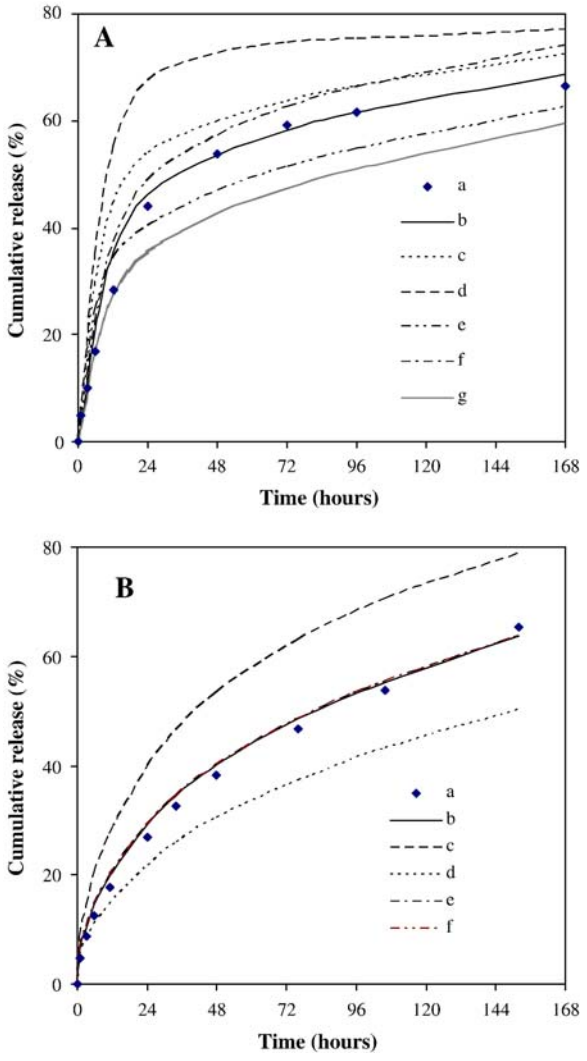

Fig. 7. Model simulation of the drug release rate from millirods. The model-simulated data were acquired by using the parameters given in Tables 1 and 2. Only one parameter was changed during each simulation. Panel A) was obtained from the HPβ–CD mixture in Fig. 3, a) experiment b) model simulation c) $2\gamma_{\beta,s}$ d) $2C_{\beta}^{max}$ e) $2\beta_{\beta c}$ f) $2\beta_{\beta}$ g) $0.5k_1/k_2$. Effects of parameters on the drug release rate were investigated, including the diffusion of drug and bound drug as well as excipient, drug and excipient dissolution process, drug complexation. Panel B) was obtained from γ–CD system in Fig. 4 to study the effects of drug re-crystallization and dissolution on drug release, a) experiment b) model simulation c) $2C_{\beta}^{thresh}$ d) $0.5C_{\beta}^{thresh}$ e) $0.5\gamma_{\beta}$ f) $2\gamma_{\beta}$. The effects of some parameters on the drug release rate were insignificant, including water penetration, entrapped drug, bound drug dissolution, forward reaction constant, etc.

HPβ–CD/β-lap solid complex incorporated into the millirods were simulated as well (Fig. 5) using parameter values estimated from other experiments. With drug loading of 3%, the drug release rate is fast; at 6% and 10%, however, the drug release rate is drastically reduced. For better simulation of the data from 6% and 10% drug loadings, the fraction parameter (F_β^*) was changed by 60% and 70%, respectively; D_β^* was reduced to 10^{-7} cm^2 h^{-1}; and the maximum water concentration was reduced by 50%.

4.3. Comparison of drug-release models

The simpler Higuchi model assumes that the accumulative drug release rate is proportional to the square root of the time (i.e., diffusion-controlled drug release rate) [24]. Without an excipient or with glucose, γ–CD, or α–CD as excipients, the Higuchi model is satisfactory (Fig. 6). In contrast, the Higuchi model cannot accurately describe release data from the HPβ–CD system. Also, the Higuchi model fails at higher drug loadings (3%, 6% and 10%).

4.4. Effects of key parameters

Simulations were made to determine the sensitivity of the drug release rate to changes in key parameters (Fig. 7). The drug release rate is sensitive to changes in values of parameters associated with drug solubility (C_β^{max}), dissolution ($\gamma_{\beta,s}$), complex binding (k_1/k_2), free drug and bound drug diffusion (β_β, $\beta_{\beta e}$), and drug threshold concentration for recrystallization (C_β^{thresh}). Parameters associated with water penetration (α), CD or complex solubility and dissolution etc. have much less effect on the drug release rate (not shown). However, under special conditions, parameters such as the solubility of the β–CD excipient may have an impact on the drug release rate.

5. Discussion

5.1. Modeling of drug release from polymeric matrices

Various models have been developed to quantify drug release from polymeric matrices. The Higuchi model [24], which assumes a pseudo-steady state, constant diffusivity, rapid drug dissolution, and sink conditions, is not applicable (1) when the initial drug concentration is lower than the drug solubility in the system; (2) during swelling or dissolution of the polymer carrier [25]. Other investigators have modeled drug release based on the dynamics of a one-dimensional concentration distribution in the matrix with various geometries or structures [26–35]. A modification of these models incorporates the dissolution process for a slowly dissolved crystalline drug [27,32]. Models have been applied to study the drug release from expandable matrices consisting of hydropropylmethylcellulose (HPMC) or polyethylene glycol (PEG) [25,36,37]. Also, the Higuchi model has been used to simulate the drug release from tablets prepared by direct compression and hot-melt extrusion [38]. This study focuses on mathematic modeling of drug release from PLGA cylindrical millirods made by compression heat-molding method. The mechanistic modeling is distinctive with respect to the drug release processes in the millirod with the β-lap drug or the drug–CD complex.

5.2. Parameter estimates

Model simulations compared most closely with various cyclodextrin systems combined with a drug loading up to 3%. However, to simulate the release kinetics of systems with no excipient, glucose, or high loading HPβ–CD, some parameter values had to be adjusted. This may be due to some simple assumptions made as well as the ignorance of some of the key processes in this modeling study.

From sensitivity analysis, parameters α, k_1, γ_β do not affect the ultimate drug release kinetics significantly (Fig. 7). Consequently, their values were fixed. For modeling drug release, we expect that water penetration precedes drug/excipient diffusion. To obtain a fast water penetration rate into millirods, we set a relatively high value for α(= 5.0×10^{-6} cm^5 h^{-1} mg^{-1}). Also, a relatively high value of γ_β(= 2.0×10^{3} h^{-1}) was set because the recrystallization process usually occurs quickly as long as C_β^{thresh} is reached. Based on the Higuchi model of the HPβ–CD complex systems, we set F_1^*(= 0.3, the intersection value) to be approximately the same. For simplicity, the threshold for recrystallization (C_β^{thresh}) was fixed to be 0.11 mg/ml based on model simulation and sensitivity studies.

As shown in Table 2, the estimated D_β^* for the drug entrapped or dissolved in the polymer matrix was either 2.6×10^{-6} or 4.5×10^{-7} cm^2 h^{-1} depending on the drug status (complex or crystalline form) in the matrix composition. This corresponds to the range (10^{-6}–10^{-8} cm^2 h^{-1}) of other drug diffusion coefficients from a PLGA matrix [34,39–41]. Water and drug diffusion coefficients in the aqueous medium are much higher (10^{-2}–10^{-3} cm^2 h^{-1}) [42,43]. For example, the diffusion coefficient of glucose (at 25 °C) in water is 2.5×10^{-2} cm^2 h^{-1} [44]. Similarly, drug diffusion coefficients in the fully swollen tablets made from HPMC or PEG, are 10^{-2}–10^{-3} cm^2 h^{-1} [37,45]. Taking into consideration of the tortuosity within discs [26,31,38], the millirods prepared by heat-melted compression have reduced diffusion coefficients β_β and $\beta_{\beta e}$ ($\sim10^{-4}$ cm^2 h^{-1}) compared to those in aqueous medium. These estimated values are close to the diffusion coefficient of theophylline from a stearic acid delivery system prepared by heat extrusion in which the porosity is around 40% [30].

The estimated binding constants (k_1/k_2) are relatively small compared with those measured at 25 °C [17]. This may be attributed to the higher experimental temperatures (37 °C) in our study [46]. For most optimally estimated parameters, the standard deviations and correlation coefficients are relatively small, which indicates that the precision of the parameter estimates is high.

5.3. Drug diffusion and matrix porosity

For excipient-free millirods (porosity = 0.05), the low drug diffusion rate coefficient (β_β = 8.4×10^{-7} cm^2 h^{-1}) correlated with the slowest drug release (Fig. 3). Glucose-containing millirods, however, showed an increased β_β, associated with a

faster release rate. Despite the comparable porosity of millirods with glucose, the millirods containing HPβ–CD/β-lap mixture produced a faster drug release rate [18]. The high forward reaction constant ($k_1 = 2 \times 10^3$ M^{-1} h^{-1}) indicates instantaneous and *in situ* formation of the complex within the millirods. k_1 was reported to be 10^8–10^7 M^{-1} s^{-1} [46]. However, our sensitivity analysis by model simulation shows that the drug release rate is reduced with decreased k_1, but does not change significantly when k_1 is further increased.

From model simulations, the contributions of free drug and bound drug to the total drug release kinetics were assessed for millirods containing HPβ–CD complex or mixture. Although the free drug contributes more in the millirods containing HPβ–CD mixture (especially in the later phase of drug release), most drug release is attributable to the complex components in both cases. Thus, incorporation of CDs can effectively modulate the drug release rate from millirods by forming an inclusion complex and increasing drug solubility. This correlates well with our sensitivity study that shows parameters associated with the complex reaction process contribute more to the drug release. The diffusion coefficient β_β of the unbound drug is higher than that of the complex-drug, whose molecular size is larger [47]. Nevertheless, a faster drug release rate is achieved from millirods containing the complex rather than in the mixture formulation because of the dominant contribution from the complexed drug (≥ 90%). Also, the glucose-containing millirod has a lower β_β than HPβ–CD-containing millirod (Table 2). This may be produced by the interactions among the crystalline drug, PLGA, and glucose. Water uptake and weight loss measurements showed a relatively slow glucose loss (data not shown), which may be associated with lower porosity and diffusivity. Increased millirod density as well as tortuosity caused by interactions among components may also contribute. In contrast, in a millirod containing HPβ–CD complex, fewer interactions exist between the complexed drug and PLGA as revealed by DSC studies [18].

5.4. Effects of excipient complexes

Significant difference in drug release rates was observed when different CD complexes were incorporated into the millirods (Fig. 4). Despite the comparable association constant of HPβ–CD to β–CD [17], millirods with HPβ–CD had a higher rate of drug release than those with β–CD, which has a lower water solubility (30.6 mg/ml). In millirods with γ–CD, which has a considerably higher water solubility (406 mg/ml), but a diffusion constant comparable to β–CD, drug release rate was lower. Model simulations showed that the binding processes in the aqueous medium made this difference. Upon contact with water, the amorphous complex in the millirods can form dissolved free drug, which may crystallize when exceeding a threshold concentration (0.11 mg/ml). The low binding constant of γ–CD complex tends to increase the free drug concentration and cause the *in situ* and quick formation of more crystalline drug within the millirods, leading to a reduced drug release rate. This result from model simulation is consistent with experiments in which drug crystallized during the dissolution of the sugar glass-based solid dispersions at increased drug loadings [48]. When the free drug concentration in the millirod is lowered below the threshold, the formed solid drug starts to dissolve and release. With crystalline drug in the α–CD complex (~50% β-lap) and its lower binding constant relative to γ–CD, the slowest drug release rate is obtained in the millirods containing α–CD.

The drug solubility (and threshold value) estimated in this study (0.11 mg/ml) is higher than that measured in water (0.04 mg/ml). This indicates the existence of super-saturation of free drug within the millirods as indicated by other studies [48]. The super-saturation of the free drug may result from high cyclodextrin concentrations within millirods, which could prevent drug crystallization above its normal solubility.

5.5. Effect of drug loading and entrapment/dissolution in PLGA matrix

Our model successfully simulated the effects of drug loadings (3, 6, 10%) as shown in Fig. 5. However, for 6% and 10% drug loading, the fraction (F_β^*) of drug dissolution/entrapped in PLGA matrix was higher. With higher loading, the amount of excipient cannot ensure the complete formation of drug inclusion complexes; consequently, the value of F_β^* will increase. In the meantime, the increased chance of drug–polymer interaction may reduce the D_β^*. DSC studies showed that the apparent drug entrapment/dissolution into PLGA decreased with the use of less CD in CD inclusion complexes [18]. Contrary to the usual expectations based on other studies [4], the drug release rate was decreased with higher drug loading (Fig. 5). This can be explained by the higher entrapment/dissolution fraction, more crystalline drug in the millirods and the reduced porosity formed during the release. Increased millirod density and tortuosity caused by higher drug loadings may also contribute to the reduced drug release.

According to our model, drug dissolved within the PLGA matrix cannot be released from a millirod as quickly as drug release via pores (with a diffusivity difference of 2–3 orders of magnitude). Without incorporating this slow process, drug release from a millirod with HPβ–CD complex would be complete within 24 h, which is not true experimentally. However, additional experiments (data not shown) using millirods with 60% CD complex showed that complete drug release required only 2 weeks.

5.6. Model comparison

The Higuchi model can be applied to simulate drug release from millirods containing glucose, or γ–CD complex, or α–CD complex, or no excipient (Fig. 6). In the excipient-free millirod, drug release is diffusion controlled. For the glucose containing millirods, the pores created by the glucose dissolution and diffusion allows water to penetrate easily into the millirods. The low binding constant of α–CD complex and γ–CD complex caused the formation of solid crystalline drug in the millirods upon their contact with water. With the α–CD complex, crystalline drug was present in the solid complex before

incorporation into the millirods. The dominant presence of crystalline drug in the millirods during the release process may determine the diffusion-controlled drug release.

The Higuchi model failed to describe the drug release dynamics for HPβ–CD (including higher loading formulations) and β–CD system as is evident when drug released is plotted versus the square-root of time. In this format, the dynamics appear to have two distinct phases. We can interpret this response based on key processes of our model. In the earlier, faster release phase, dissolution of the cyclodextrin excipient or complex, pore formation and their subsequent rapid diffusion via pores are dominant. In the later, slower release phase, drug comes from the fraction that is dissolved/entrapped in the PLGA matrix.

To further examine the range of validity of the Higuchi model [24], we applied it with the parameters from our model to simulate drug release rate from the millirods. For millirods containing glucose, no-excipient and α–CD complex, the Higuchi model predicted a faster release than the experimental data. This discrepancy is likely due to kinetic processes such as water penetration and drug dissolution that are not included in the Higuchi model, which may delay the drug release rate assuming the same drug diffusion coefficient. From γ–CD-containing millirods, however, the drug release rate predicted by the Higuchi model was slower than observed experimentally. This may be caused by the failure of Higuchi model to deal with the complexed drug as well as the drug dissolved/entrapped in the PLGA matrix, which is relatively low and ignorable in glucose and α–CD millirods. Whereas the Higuchi model provides a successful description of the drug release under some conditions, our model can predict drug release under more general conditions by incorporation of key underlying mechanisms.

5.7. Model limitations and future work

Overall our mechanistic model for drug release from millirods can simulate a variety of experimental conditions. However, assuming that the water penetration coefficient is identical for all millirod compositions may be incorrect because of solubility differences and drug/excipient interactions with PLGA. Also, the correlation of the porosity with water penetration and the drug/excipient dissolution may not be as simple as represented. Especially, at higher drug loadings, the use of much less soluble excipient and more crystalline drug may have resulted in decreased porosity and diffusivity, which our model did not take into account. Improvements in this model can be made with additional experiments to quantitatively characterize water penetration rate and millirod weight loss, or by directly measuring some key parameters (e.g. k_1, k_2, drug/complex diffusivities in PBS at 37 °C). Future studies should examine excipient levels other than 40% that would significantly affect the drug release rate as well.

6. Conclusions

A mechanistic model has been developed to analyze and predict drug release kinetics from the millirods that incorporate various excipients, viz., glucose and cyclodextrins. This model was validated by comparison with drug release experiments under a variety of conditions. Optimal estimates of the parameters were obtained by comparing model simulations of drug release with corresponding experimental data. Our model can simulate all the experimental data whereas the Higuchi model can simulate only some of them. Furthermore, our model provided insights into the complex-loaded millirod systems and revealed mechanisms by which the processes underlying drug release from a polymer matrix can be quantitatively analyzed. These processes include entrapment/dissolution of drug in the matrix, drug recrysallization, and supersaturation.

Acknowledgements

The authors would like to thank Dr. Zhenghong Lee for his support during the completion of this project. We also thank Dr. David Boothman for helpful discussions. This work is supported by the National Institutes of Health (R01 CA90696 to J.G.).

References

[1] D.A. LaVan, T. McGuire, R. Langer, Small-scale systems for in vivo drug delivery, Nat. Biotechnol. 21 (10) (2003) 1184–1191.
[2] F. Qian, A. Szymanski, J.M. Gao, Fabrication and characterization of controlled release poly(D,L-lactide-co-glycolide) millirods, J. Biomed. Mater. Res. 55 (4) (2001) 512–522.
[3] F. Qian, G.M. Saidel, D.M. Sutton, A. Exner, J.M. Gao, Combined modeling and experimental approach for the development of dual-release polymer millirods, J. Control. Release 83 (3) (2002) 427–435.
[4] F. Qian, N. Nasongkla, J.M. Gao, Membrane-encased polymer millirods for sustained release of 5-fluorouracil, J. Biomed. Mater. Res. 61 (2) (2002) 203–211.
[5] F. Qian, N. Stowe, G.M. Saidel, J.M. Gao, Comparison of doxorubicin concentration profiles in radiofrequency-ablated rat livers from sustained- and dual-release PLGA millirods, Pharm. Res. 21 (3) (2004) 394–399.
[6] F. Qian, N. Stowe, E.H. Liu, G.M. Saidel, J.M. Gao, Quantification of in vivo doxorubicin transport from PLGA millirods in thermoablated rat livers, J. Control. Release 91 (1–2) (2003) 157–166.
[7] B. Weinberg, H. Ai, E. Blanco, J. Anderson, J. Gao, Antitumor efficacy and local pharmacokinetics of doxorubicin via intratumoral delivery from polymer millirods, J. Biomed. Mater. Res. 81 (1) (2007) 161–170.
[8] E. Blanco, B.D. Weinberg, N.T. Stowe, J.M. Anderson, J. Gao, Local release of dexamethasone from polymer millirods effectively prevents fibrosis after radiofrequency ablation, J. Biomed. Mater. Res. A 76 (1) (2006) 174–182.
[9] J.J. Pink, S. Wuerzberger-Davis, C. Tagliarino, S.M. Planchon, X.H. Yang, C.J. Froelich, D.A. Boothman, Activation of a cysteine protease in MCF-7 and T47D breast cancer cells during beta-lapachone-mediated apoptosis, Exp. Cell Res. 255 (2) (2000) 144–155.
[10] M. Ough, A. Lewis, E.A. Bey, J.M. Gao, J.M. Ritchie, W. Bornmann, D.A. Boothman, L.W. Oberley, J.J. Cullen, Efficacy of beta-lapachone in pancreatic cancer treatment — exploiting the novel, therapeutic target NQO1, Cancer Biol. Ther. 4 (1) (2005) 95–102.
[11] J.J. Pink, S.M. Planchon, C. Tagliarino, M.E. Varnes, D. Siegel, D.A. Boothman, NAD(P)H: quinone oxidoreductase activity is the principal determinant of beta-lapachone cytotoxicity, J. Biol. Chem. 275 (8) (2000) 5416–5424.
[12] D. Siegel, D. Ross, Immunodetection of NAD(P)H:quinone oxidoreductase 1 (NQO1) in human tissues, Free Radic. Biol. Med. 29 (3–4) (2000) 246–253.
[13] C. Tagliarino, J.J. Pink, K.E. Reinicke, S.M. Simmers, S.M. Wuerzberger-Davis, D.A. Boothman, mu-calpain activation in beta-lapachone-mediated apoptosis, Cancer Biol. Ther. 2 (2) (2003) 141–152.

[14] S.M. Planchon, S. Wuerzberger, B. Frydman, D.T. Witiak, P. Hutson, D.R. Church, G. Wilding, D.A. Boothman, Beta-lapachone-mediated apoptosis in human promyelocytic leukemia (HL-60) and human prostate cancer cells: a p53-independent response, Cancer Res. 55 (17) (1995) 3706–3711.
[15] C.J. Li, Y.Z. Li, A.V. Pinto, A.B. Pardee, Potent inhibition of tumor survival in vivo by beta-lapachone plus taxol: combining drugs imposes different artificial checkpoints, Proc. Natl. Acad. Sci. U. S. A. 96 (23) (1999) 13369–13374.
[16] D.A. Boothman, I. Bouvard, E.N. Hughes, Identification and characterization of X-Ray-induced proteins in human-cells, Cancer Res. 49 (11) (1989) 2871–2878.
[17] N. Nasongkla, A.F. Wiedmann, A. Bruening, M. Beman, D. Ray, W.G. Bornmann, D.A. Boothman, J.M. Gao, Enhancement of solubility and bioavailability of beta-lapachone using cyclodextrin inclusion complexes, Pharm. Res. 20 (10) (2003) 1626–1633.
[18] F.J. Wang, E. Blanco, H. Ai, D.A. Boothman, J.M. Gao, Modulating beta-lapachone release from polymer millirods through cyclodextrin complexation, J. Pharm. Sci. 95 (2006) 2309–2319.
[19] T. Loftsson, Cyclodextrins and the biopharmaceutics classification system of drugs, J. Incl. Phenom. Macro 44 (1–4) (2002) 63–67.
[20] J. Szejtli, Introduction and general overview of cyclodextrin chemistry, Chem. Rev. 98 (5) (1998) 1743–1754.
[21] V.R. Sinha, R. Anitha, S. Ghosh, A. Nanda, R. Kumria, Complexation of celecoxib with beta–cyclodextrin: characterization of the interaction in solution and in solid state, J. Pharm. Sci. 94 (3) (2005) 676–687.
[22] K. Okimoto, R.A. Rajewski, V.J. Stella, Release of testosterone from an osmotic pump tablet utilizing (SBE)(7m)-beta-cyclodextrin as both a solubilizing and an osmotic pump agent, J. Control. Release 58 (1) (1999) 29–38.
[23] M.J. Jozwiakowski, K.A. Connors, Aqueous solubility behavior of three cyclodextrins, Carbohydr. Res. 143 (1985) 51–59.
[24] T. Higuchi, Rate of release of medicaments from ointment bases containing drugs in suspension, J. Pharm. Sci. 50 (10) (1961) 874–875.
[25] J. Siepmann, N.A. Peppas, Modeling of drug release from delivery systems based on hydroxypropyl methylcellulose (HPMC), Adv. Drug Deliv. Rev. 48 (2–3) (2001) 139–157.
[26] C.H. Wang, K. Sengothi, T. Lee, Controlled release of human immunoglobulin G. 1. Release kinetics studies, J. Pharm. Sci. 88 (2) (1999) 215–220.
[27] G. Frenning, Theoretical investigation of drug release from planar matrix systems: effects of a finite dissolution rate, J. Control. Release 92 (3) (2003) 331–339.
[28] N.A. Peppas, P.L. Ritger, A simple equation for description of solute release 1. Fickian and non-Fickian release from non-swelllable devices in the form of slabs, spheres, cylinders or discs, J. Control. Release 5 (1987) 23–36.
[29] N.A. Peppas, J.J. Sahlin, A simple equation for the description of solute release.3. Coupling of diffusion and relaxation, Int. J. Pharm. 57 (2) (1989) 169–172.
[30] M. Grassi, D. Voinovich, E. Franceschinis, B. Perissutti, J. Filipovic-Grcic, Theoretical and experimental study on theophylline release from stearic acid cylindrical delivery systems, J. Control. Release 92 (3) (2003) 275–289.
[31] M.P. Zhang, Z.C. Yang, L.L. Chow, C.H. Wang, Simulation of drug release from biodegradable polymeric microspheres with bulk and surface erosions, J. Pharm. Sci. 92 (10) (2003) 2040–2056.
[32] G. Frenning, Theoretical analysis of the release of slowly dissolving drugs from spherical matrix systems, J. Control. Release 95 (1) (2004) 109–117.
[33] Y. Zhou, X.Y. Wu, Modeling and analysis of dispersed-drug release into a finite medium from sphere ensembles with a boundary layer, J. Control. Release 90 (1) (2003) 23–36.
[34] M. Hombreiro-Perez, J. Siepmann, C. Zinutti, A. Lamprecht, N. Ubrich, M. Hoffman, R. Bodmeier, P. Maincent, Non-degradable microparticles containing a hydrophilic and/or a lipophilic drug: preparation, characterization and drug release modeling, J. Control. Release 88 (3) (2003) 413–428.
[35] M. Polakovic, T. Gorner, R. Gref, E. Dellacherie, Lidocaine loaded biodegradable nanospheres II. Modelling of drug release, J. Control. Release 60 (2–3) (1999) 169–177.
[36] S. Kiil, K. Dam-Johansen, Controlled drug delivery from swellable hydroxypropylmethylcellulose matrices: model-based analysis of observed radial front movements, J. Control. Release 90 (1) (2003) 1–21.
[37] N. Wu, L.S. Wang, D.C.W. Tan, S.M. Moochhala, Y.Y. Yang, Mathematical modeling and in vitro study of controlled drug release via a highly swellable and dissoluble polymer matrix: polyethylene oxide with high molecular weights, J. Control. Release 102 (3) (2005) 569–581.
[38] M.M. Crowley, B. Schroeder, A. Fredersdorf, S. Obara, M. Talarico, S. Kucera, J.W. McGinity, Physicochemical properties and mechanism of drug release from ethyl cellulose matrix tablets prepared by direct compression and hot-melt extrusion, Int. J. Pharm. 269 (2) (2004) 509–522.
[39] N. Faisant, J. Siepmann, J. Richard, J.P. Benoit, Mathematical modeling of drug release from bioerodible microparticles: effect of gamma-irradiation, Eur. J. Pharm. Biopharm. 56 (2) (2003) 271–279.
[40] J. Siepmann, N. Faisant, J. Akiki, J. Richard, J.P. Benoit, Effect of the size of biodegradable microparticles on drug release: experiment and theory, J. Control. Release 96 (1) (2004) 123–134.
[41] R.T. Kurnik, R.O. Potts, Modeling of diffusion and crystal dissolution in controlled release systems, J. Control. Release 45 (3) (1997) 257–264.
[42] K.C. Sung, E.M. Topp, Effect of drug hydrophilicity and membrane hydration on diffusion in hyaluronic-acid ester membranes, J. Control. Release 37 (1–2) (1995) 95–104.
[43] J.E. Hastedt, J.L. Wright, Diffusion in porous materials above the percolation-threshold, Pharm. Res. 7 (9) (1990) 893–901.
[44] T. Koizumi, G.C. Ritthidej, T. Phaechamud, Mechanistic modeling of drug release from chitosan coated tablets, J. Control. Release 70 (3) (2001) 277–284.
[45] J. Siepmann, K. Podual, M. Sriwongjanya, N.A. Peppas, R. Bodmeier, A new model describing the swelling and drug release kinetics from hydroxypropyl methylcellulose tablets, J. Pharm. Sci. 88 (1) (1999) 65–72.
[46] V.J. Stella, V.M. Rao, E.A. Zannou, V. Zia, Mechanisms of drug release from cyclodextrin complexes, Adv. Drug Deliv. Rev. 36 (1) (1999) 3–16.
[47] D.C. Bibby, N.M. Davies, I.G. Tucker, Mechanisms by which cyclodextrins modify drug release from polymeric drug delivery systems, Int. J. Pharm. 197 (1–2) (2000) 1–11.
[48] D.J. van Drooge, W.L.J. Hinrichs, H.W. Frijlink, Anomalous dissolution behaviour of tablets prepared from sugar glass-based solid dispersions, J. Control. Release 97 (3) (2004) 441–452.